Materials for life sciences

Biphasic scaffolds of polyvinyl alcohol with silk fibroin for oral and maxillofacial surgery based on mimicking materials design: fabrication, characterization, properties

Tanchanok Parivatphun[1], Supaporn Sangkert[2], Rungrote Kokoo[3], Matthana Khangkhamano[1], and Jirut Meesane[2,*] (iD)

[1] *Department of Mining and Material Engineering, Faculty of Engineering, Prince of Songkla, Songkhla, Thailand*

[2] *Institute of Biomedical Engineering, Prince of Songkla University, Hat Yai, Songkhla 90112, Thailand*

[3] *Department of Chemical Engineering, Faculty of Engineering, King Mongkut's University of Technology, North Bangkok 10800, Thailand*

ABSTRACT

Biphasic scaffolds were created based on mimicking materials design and evaluated to identify certain applications for oral and maxillofacial surgery. Polyvinyl alcohol (PVA) and different amounts of silk fibroin (SF)—0%, 1%, 3%, and 5% (PVA, PVA/1% SF, PVA/3% SF, and PVA/5% SF)—were used to fabricate biphasic scaffolds via the micro-bubble approach before freeze-thawing and freeze-drying. These scaffolds were characterized and their molecular organization and morphology were observed using Fourier transform infrared (FTIR) spectroscopy and scanning electron microscopy (SEM), respectively. The performance of the scaffolds was tested in terms of their swelling behavior and mechanical properties. They were cultured with MC3T3E1 osteoblast cells and L929 fibroblast cells. The main biological performance of cell proliferation was analyzed. The molecular organization of the fabricated biphasic scaffolds possessed interaction and mobility properties via the –OH and the amide I, II, and III groups. Their morphology demonstrated pores with fibrils. They showed a high level of performance in terms of swelling, mechanical strength, and cell proliferation. Finally, based on the findings of this research, it can be deduced that PVA/5% SF can provide a suitable biphasic scaffold with high promise for oral and maxillofacial surgery for instance mandibular ridge augmentation and repair of alveolar cleft lip and palate.

Springer

Introduction

Many patients suffer from bone defects at the oral maxillofacial area [1]. In severe cases, patients benefited from effective biomaterial implantations at the defect site [2, 3]. However, biomaterials for implantation need to be biocompatible and non-toxic [4, 5]. Some materials scientists and surgeons have created good performance biomaterials to promote new tissue formation at a defect site that is suitable as a surgical approach [6]. Therefore, it is a challenge to develop biomaterials that merge bioperformance and surgical requirements, especially for surgery in the oral and maxillofacial area.

Tissue engineering scaffolds are effective biomaterials, which are often used in the treatment of patients that suffer from a tissue defect due to disease or trauma [7, 8]. They are often used to enhance new tissue formation in large defects [9–11]. Interestingly, some previous research proposed scaffolds as performance biomaterials to enhance new tissue formation at a defect area for oral and maxillofacial surgery. In some cases, surgeons have used both two-dimensional (2D) and three-dimensional (3D) scaffolds to complete surgery. However, the surgery is complicated and it is important to reduce the risk of infection during surgery [12, 13]. Therefore, it is necessary to design novel scaffolds that support biological functions, avoid infection, and meet the requirements for surgical applications.

Biphasic scaffolds are often created for defect areas that include two types of tissue [14]. For instance, biphasic scaffolds are used in osteoarthritis, which involves defects of both bone and cartilage tissue [15]. Another example is a biphasic scaffold created for an anterior cruciate ligament, which contacts the bone [16]. Therefore, biphasic scaffolds are fabricated to promote tissue formation at defect sites that have the complicated structure of two phases, which are the soft tissue and bone tissue. Biphasic scaffolds can reduce the surgical time that minimizes the risk of infection. Furthermore, biphasic scaffolds can facilitate new tissue formation and maintain the contour shape of the defect area until repair is complete. So far, few reports are available regarding biphasic scaffolds fabricated for oral and maxillofacial surgery in contact with both soft tissue and bone tissue [14, 15]. In this research, biphasic scaffolds were fabricated as performance biomaterials for the novel function of tissue repair in oral and maxillofacial surgery.

An attractive approach to fabricating performance scaffolds is mimicking, which has been used to design innovative materials for mechanical engineering [17, 18], nanotechnology [19], and materials science and engineering [19], to name a few. Mimicking is applied to create desired structures, mechanical properties, fabrication process, and performance. In the case of materials for bone augmentation, many materials have been fabricated into 2D scaffolds with structures and functions similar to regenerative tissue [9]. For example, 2D scaffolds were fabricated into a mimicked structure similar to soft tissue for bone augmentation [20]. Other scaffolds were created into 3D porous structures with components that provided biological characteristics similar to the extracellular matrix (ECM) of tissue [21]. 3D scaffolds are also used as biomaterials for oral and maxillofacial surgery. However, little research has reported on biphasic scaffolds based on mimicking materials design suitable for the two-phase environment of a tissue defect at the oral and maxillofacial area [14].

Polyvinyl alcohol (PVA) is a synthetic polymer, which is used in the creation of biomaterials; some of its applications are in the areas of artificial skin and cartilage [22]. Since PVA possess a good thermoplastic performance, it can be processed into various forms [23]. Furthermore, due to its biocompatibility, non-toxicity, biodegradability, and hydrophilicity, PVA is suitable for tissue engineering of scaffolds [24]. PVA is often blended with other polymers to enhance its toughness giving it suitable mechanical properties for the engineering of bone tissue scaffolds [22, 25]. Since PVA has a non-biological function, organic or inorganic molecules, which have important roles in enhancing bone formation, are added to PVA, for instance, collagen, gelatin, hydroxyapatite, β-tricalcium phosphate, and titanium oxide [26, 27]. These molecules are normally mixed with PVA before fabrication into different scaffolds with different techniques, for example freeze-drying, particle leaching, electro-spinning, solution casting, and micro-bubble [28, 29]. Some studies report that PVA scaffolds with biomolecules were fabricated with adapted techniques to form structures and geometries that would be suitable for the proposed application. For instance, some research presented adaptation of particle deposition incorporated with

the layer-by-layer technique to fabricate PVA membrane scaffolds [30]. In this research, PVA was selected as the base material for fabrication with an adapted technique suitable for biphasic scaffolds.

Silk fibroin (SF) is a natural polymer, which is used in various biomaterial applications [31]. As is the case with PVA, due to its biocompatibility, non-toxicity, and biodegradability, SF is often used in the tissue engineering of scaffolds [32]. Interestingly, SF possesses amino acids that act as binding sites for cell adhesion, which gives it a good osteo-conductive performance [33]. Furthermore, SF has three structural forms: 1) random coil, 2) alpha helix, and 3) beta sheet [34]. Each form has different properties that affect the performance of biomaterials [35]. For bone tissue engineering, SF organized as a beta sheet structure has been selected often as the base material for scaffolds due to its dense structure that has a greater effect on physical and mechanical stability than the other forms [36, 37]. Therefore, SF is often used in the engineering of bone tissue scaffolds [38]. Importantly, SF scaffolds have the physical properties and biological functions suitable for maintaining the contour shape and promote new bone tissue at a defect site [20, 39]. Based on the good points of SF, it was selected to be incorporated with the PVA base in the fabrication of biphasic scaffolds in this research.

Mimicked biphasic scaffolds are often fabricated with the assembly of two monophasic scaffolds into different geometries [40]. For our scaffolds, we present an alternative choice for fabrication. The scaffolds formed a biphasic structure via self-organization during fabrication. In this research, biphasic scaffolds were created based on mimicking materials design using the micro-bubble technique incorporated with freeze-drying before methanol treatment. For fabrication, PVA was blended with different amounts of SF into a solution, which was then fabricated into the biphasic scaffolds. The mixed solution with micro-bubbles was poured into a mold to prepare the samples, which were then freeze-dried to form the biphasic scaffolds before methanol treatment. The obtained biphasic scaffolds were characterized, and the biological response of cells was investigated. Finally, the scaffolds were evaluated for their potential in oral and maxillofacial surgery.

Materials and methods

Preparation of the silk fibroin solution

The silk fibroin (SF) was provided by the Queen Sirikit Sericulture Center, Narathiwat, Thailand. The SF solution was prepared according to the protocol proposed by Panjapheree et al. [14]. Initially, the SF fibers were heated in a 0.02 M solution of sodium carbonate (Na_2CO_3) for 20 min and then washed with distilled water to remove the sericin glue before drying. The dried SF fibers were dissolved in a 9.3 M lithium bromide solution (LiBr) at 70 °C for 150 min. The SF solution was then dialyzed using distilled water for 3 days and centrifuged at 9000 rpm for 20 min. Finally, a purified SF solution was obtained. Three concentrations of SF solutions were prepared at 1%, 3%, and 5% (w/v).

Preparation of the PVA solution

The polyvinyl alcohol (PVA, Mw ≈ 47,000 g/mol, 98% hydrolyzed) was purchased from the Fluka Chemika Company. The PVA powder was dissolved in distilled water at 20% w/v and stirred at 80 °C for 75 min. The PVA solution was allowed to cool to room temperature to prevent coagulation while mixing with the SF solution.

Preparation of the 3D PVA/silk scaffolds

The design of the bubbling process is shown in Fig. 1. A bubble column with a diameter of 30 mm was firmly connected to a diffuser with a pore size of 10–16 μm (ROBU® Glasfilter-Geräte GmbH, Grade P4). The column was connected to plastic tubes, a flow meter, and an air compressor. A bubble cloud was generated as air was blown through the bubble column.

A volume of 10 ml of SF solution was loaded into the bubble column at different concentrations (1%, 3%, and 5% w/v). Air at a flow rate of 200 cc/min was fed into the column containing the SF solution to generate air bubbles within the solution. The PVA solution was then poured into the column to mix with the bubbled SF solution as the air was flowing. The mixed solution was allowed to foam until it reached the maximum foam volume. After that, the foam was transferred to an aluminum mold and frozen at –4 °C for 12 h to form a bulk solid of a 3D
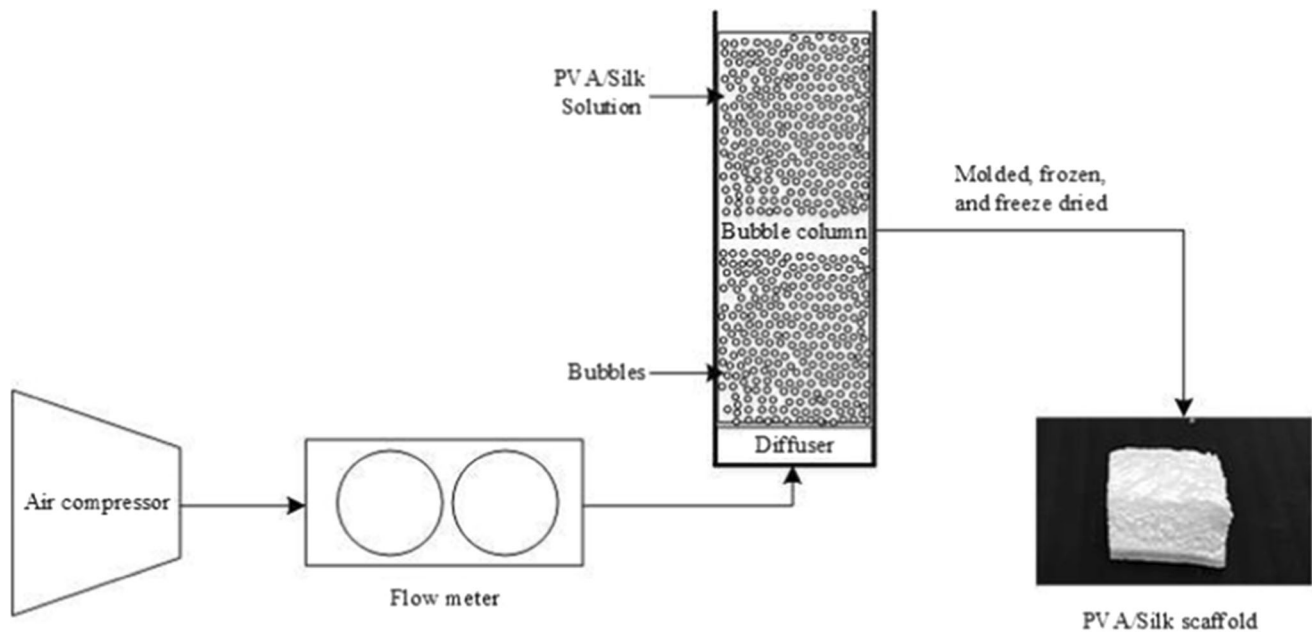
Figure 1 Experimental setup for PVA/silk scaffold fabrication via bubbling technique.

PVA/silk scaffold before thawing at room temperature for 30 min. The freeze-drying technique was then applied to form the dried PVA/silk scaffold at −96 °C for 12 h. The dried scaffold was immersed in 50% v/v methanol at room temperature to transform proteins from random coil to beta sheet structures for 10 min. Table 1 illustrates the list of samples fabricated at different concentrations of the silk solution.

Characterization

Fourier transform infrared (FTIR) spectroscopy

The molecular organization of the PVA/silk scaffolds was analyzed using a Fourier transform infrared spectrometer (FTIR, EQUNOX55, Bruker, Germany)

Table 1 List of 3D scaffold samples fabricated at various concentrations of SF solution

Scaffold samples	Concentration of SF solution(%w/v)
PVA	0% silk fibroin
PVA/1% SF	1% silk fibroin
PVA/3% SF	3% silk fibroin
PVA/5% SF	5% silk fibroin

in the ATR mode under wave numbers ranging from 4000 to 400 cm^{-1}.

Scanning electron microscopy (SEM)

The morphological study was carried out using scanning electron microscopy (SEM, JEOL, JSM-5800LV) at an accelerating voltage of 20 kV. The cell size (bubble size) was evaluated using the ImageJ software.

Swelling test

The swelling properties of the scaffolds were tested by immersion in PBS at 37 °C for different time points: 15, 30, 60, 120, 240, 480, and 960 min. Both the original and swollen weights of the scaffold were measured in order to calculate the swelling properties using the following equation: Swelling ratio = (Ws–Wd)/Wd. The Ws and Wd represented the weights of the swollen scaffold and the dry scaffold, respectively.

Mechanical testing

Compression testing was performed using a universal testing machine (Tinius Olsen, H10KS) to evaluate the compressive strength of the samples. The scaffolds were cut into a square shape of $1 \times 1 \times 1$ cm^3. The test was performed on the samples under both

dry and wet conditions. For the wet condition, the samples were soaked in a buffer solution (phosphate buffer saline [PBS]) for 24 h at room temperature. The load was 100 N at 1 mm/min. A strain limit of 0.4 mm/min (40%) was considered. The scaffold samples were subjected to a compressive load along the axis to assess the mechanical properties of the PVA/silk scaffolds. The compressive moduli were measured via the Horizon software, and a P value < 0.05 was regarded as statistically significant.

Fibroblast culturing

The L929 fibroblast cells were kept in DMEM media that consisted of 10% fetal bovine serum (FBS, Gibco, Invitrogen, USA), 1% penicillin and streptomycin (Gibco, Invitrogen, USA), and 0.1% Fungizone (Gibco, Invitrogen, USA). The cells were incubated at 37 °C in a humidified incubator at 5% CO_2 and 95% air. The cells were seeded at a density of 2×10^4 per scaffold.

Osteoblast culturing

The MC3T3E1 cells were cultured in the alpha MEM supplement with 10% fetal bovine serum (FBS, Gibco, Invitrogen, USA), 1% penicillin and streptomycin (Gibco, Invitrogen, USA), and 0.1% Fungizone (Gibco, Invitrogen, USA). The cells were then seeded at a density of 1×10^6 onto the scaffold, and the culture was incubated at 37 °C in a humidified incubator at 5% CO_2 and 95% air.

Cell proliferation

After cell seeding of the fibroblast and the osteoblast cells, cell proliferation was evaluated on days 1, 3, 5, and 7 with PrestoBlue® reagent (PrestoBlue® Cell Viability Reagent, Invitrogen, USA). The medium was removed and rinsed several times with PBS. The PrestoBlue was combined with the medium at a ratio of 1/10 and added directly to the scaffold, which was then incubated for 1 h at 37 °C. Finally, 200 ul of solution was collected in a 96-well plate, and its wavelength absorbance was measured at a 600 nm emission wavelength.

Statistical analysis

Samples were tested for their physical and mechanical properties. Culturing of the fibroblast and osteoblast cells was also evaluated. The data are presented as mean ± standard deviation. The results were statistically measured and compared by one-way ANOVA and Tukey's HDS test (SPSS 16.0 software package). P values < 0.05 were accepted as statistically significant.

Results

Macrostructure of the PVA/silk scaffolds

We aimed to design and construct a scaffold with a structure that is closely similar to the ECM in the body [25]. The ECM possesses the complex structure of proteins, which are important for cell adhesion [26]. Silk is composed of two proteins: fibroin and sericin [27]. Therefore, its structure resembles that of the ECM. Therefore, a 3D scaffold was fabricated by combining PVA and silk firoin via the bubbling process to simulate and mimic the ECM (Fig. 2). The PVA/silk scaffolds had two structures: the thin film layer and foam. The PVA solution was stable without the assistance of any other chemicals or organic solvents. Different concentrations of silk solution were used to generate the scaffold structures of various pore sizes. The dried scaffolds maintained their 3D shape without damage to their pore structure or silk shrinkage in the scaffold structure. The microstructure of the scaffolds is presented in Fig. 3.

Morphological study

Figure 3 shows the cross-sectional views of the scaffolds prepared at various concentrations of the SF solution. Cleary, all of the fabricated scaffolds exhibited two distinct structures (Fig. 3a–d). One of them is that of a layer of a highly porous and interconnected cell network structure and the other is that of a layer of thin film. It was obvious that the cellular structure had a sphere-like shape, which was uniformly covered by the SF fibers throughout the scaffold. In addition, the introduction of SF into the scaffold provided highly porous internal networks in the structure (Fig. 3e–h). As more SF was added, a more complex internal network was generated.

Figure 2 Photographs of the fabricated PVA/Silk scaffolds: **a** 0% w/v; **b** 1% w/v; **c** 3% w/v; and **d** 5% w/v.
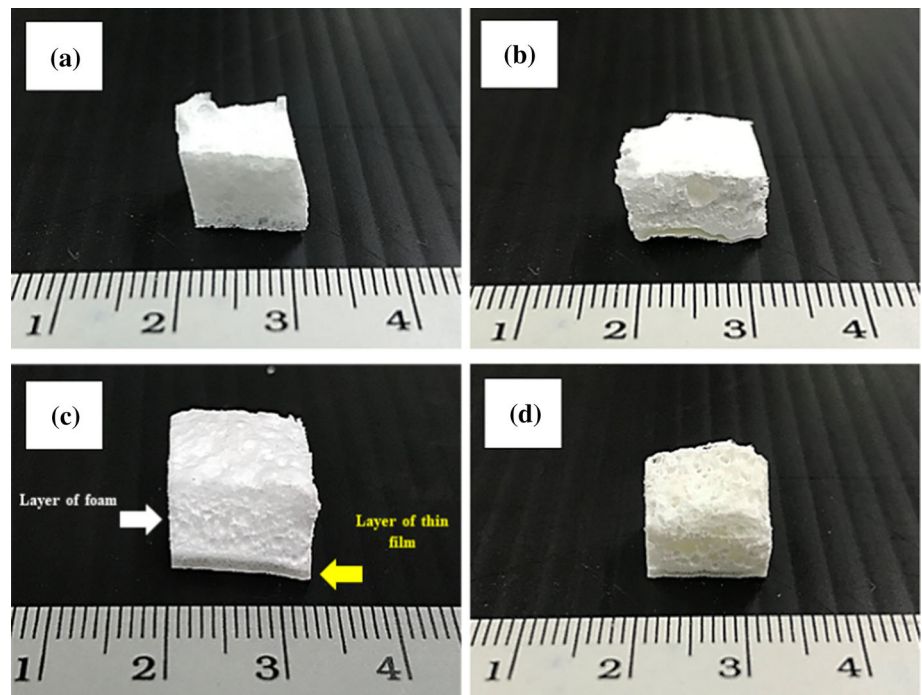
Clearly, the PVA/5% SF scaffold demonstrated a dense internal network throughout the structure.

Figure 4 shows the size distribution of sub-pores and main pores of the PVA/silk scaffold. The average sub-pore sizes of PVA/0% SF, PVA/1% SF, PVA/3% SF, and PVA/5% SF were 116.68, 113.58, 106.08, and 103.5 μm, respectively. The average main pore sizes of PVA/0% SF, PVA/1% SF, PVA/3% SF, and PVA/5% SF were 443.08, 389.04, 424.20, and 436.04 μm, respectively. Apparently, the size of the sub-pores decreased under the same flow rate as the concentration of SF increased in the solution.

FTIR spectroscopy analysis of PVA/silk scaffolds

FTIR was used to analyze the PVA/silk fibroin sponge and film structures (Fig. 5). The results are demonstrated in Figs. 5a and b. Regarding PVA, two major vibration peaks were observed at 3550–3200 cm^{-1} and 3000–2840 cm^{-1}. They were verified as O–H and C–H from the alkyl groups [28]. Three major vibration peaks for the silk were found at 1698–1622 cm^{-1}, 1540–1520 cm^{-1}, and 1258–1229 cm^{-1} belonging to the amide I (C = O stretching), amide II (N–H bending), and amide III (C–N stretching) groups, respectively [41, 42].

The film analysis results showed that PVA, PVA/1%, PVA/3%, and PVA/5% had –OH wavenumbers of around 3259, 3274, 3272, and 3276 cm^{-1}, respectively. PVA/1%, 3%, and 5% SF demonstrated amide I groups at values of around 1653, 1654, and 1646 cm^{-1}, respectively. The amide II groups of PVA/1%, 2%, and 3% SF were detected at around 1542, 1542, and 1538 cm^{-1}, respectively. In terms of the amide III groups, the wavenumbers were 1240, 1240, and 1239 cm^{-1} for PVA/1%, 3%, and 5% SF, respectively.

The sponge structure of the PVA, PVA/1%, 3%, and 5% SF showed –OH groups at around 3279, 3279, 3285, 3275 cm^{-1}, respectively. Meanwhile, the amide I groups had wavenumbers at around 1646, 1655, and 1647 cm^{-1}, respectively. The amide II values were at around 1540, 1547, 1541 cm^{-1}, respectively, and the amide III wavelengths were approximately the same at 1239 cm^{-1}.

Swelling behavior of the PVA/silk scaffolds

The swelling property of the scaffold in each group was observed between 15 and 240 min in PBS at 37 °C, and a rising trend over time was observed (Fig. 6). The pure PVA group showed the highest swelling percentage over the first 15 min, whereas the 3% SF group showed the lowest swelling

Figure 3 SEM images of the fabricated biphasic scaffolds: **a**, **e** PVA; **b**, **f** PVA/1% SF; **c**, **g** PVA/3% SF; and **d**, **h** PVA/ 5% SF. White and yellow arrows indicate the areas of film and sponge structures, respectively. The yellow circle indicates the cell structure.
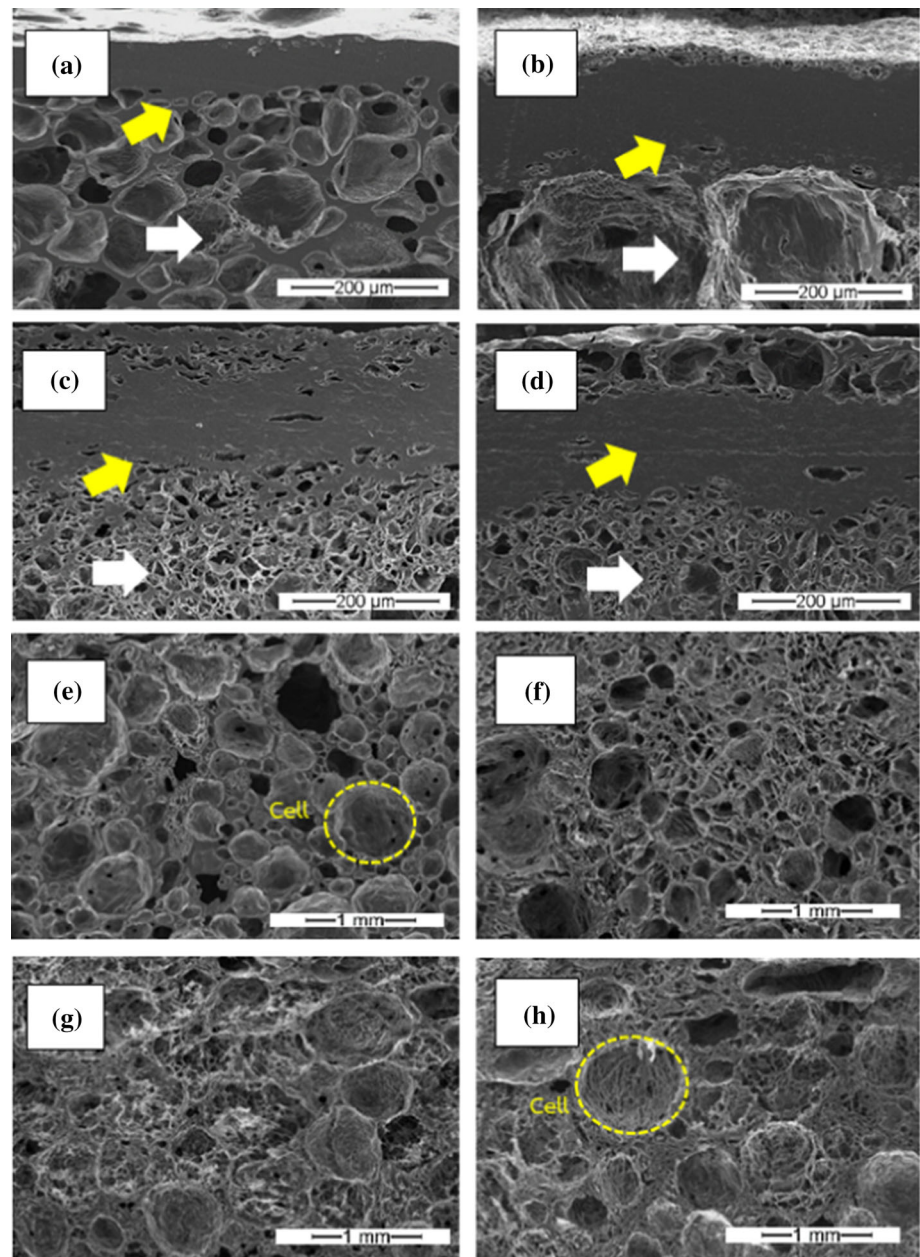
percentage. At the 30 min time point, the 5% SF overtook the pure PVA group in terms of swelling. Meanwhile, the 1% SF group continued to exhibit the lowest swelling increase of all the groups, and its swelling trend was steady until 120 min. The 5% SF group experienced the highest swelling proportion among the groups at 240 min, while the 3% SF group showed the lowest level of swelling.

Mechanical properties of the PVA/silk scaffolds

In this research, the SF was incorporated into the scaffold to improve its mechanical properties under both dry and wet environments (Fig. 7). In the dry condition (Fig. 7a), the PVA/5% SF scaffold showed a significantly higher compressive strength than the other scaffolds. The PVA/1% SF and PVA/3% SF scaffolds exhibited similar compressive strength. The results demonstrated that the compressive strength grew as the SF concentration increased. The strength
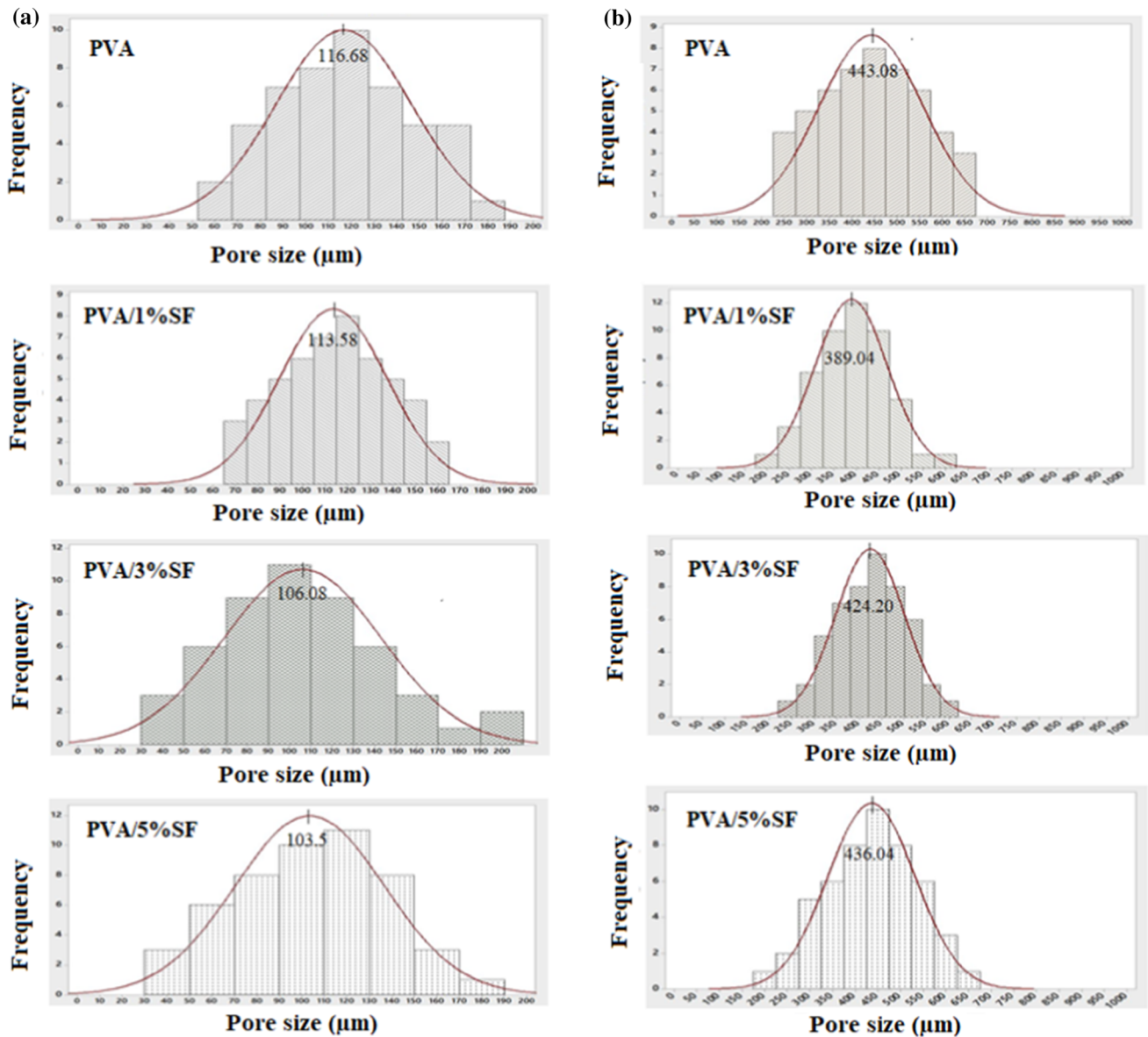
Figure 4 Size distribution of the sub-pores **a** and main pores **b** of the scaffolds according to the different amounts of silk fibroin.

of the scaffolds under a wet condition (Fig. 7c) was also analyzed to mimic the environment in the body where they would come into contact with body fluids. Once again, the PVA/5% SF scaffold expressed the highest compressive strength, whereas the PVA/3% SF scaffold showed the lowest level of strength. In the wet condition, all scaffolds presented lower compressive strengths than in the dry condition due to water absorption. The stress–strain curve of the PVA/silk scaffolds in both dry and wet environments is presented in Figs. 7b and d. In the dry condition, the scaffold with the lowest compressive strength was the PVA/3% SF scaffold, whereas in the

wet condition, the PVA/0% SF scaffold demonstrated the lowest compressive strength.

Cell proliferation of fibroblast and osteoblast cells

Cell proliferation was measured on days 1, 3, 5, and 7 using PrestoBlue reagent (Fig. 8). At day 1, the PVA scaffold showed the lowest fibroblast cell proliferation rate, and the PVA/5% SF scaffold had the highest proliferation rate (Fig. 8a). Fibroblast cell proliferations of the PVA/1% SF and PVA/3% SF scaffolds were not significantly different. Cell
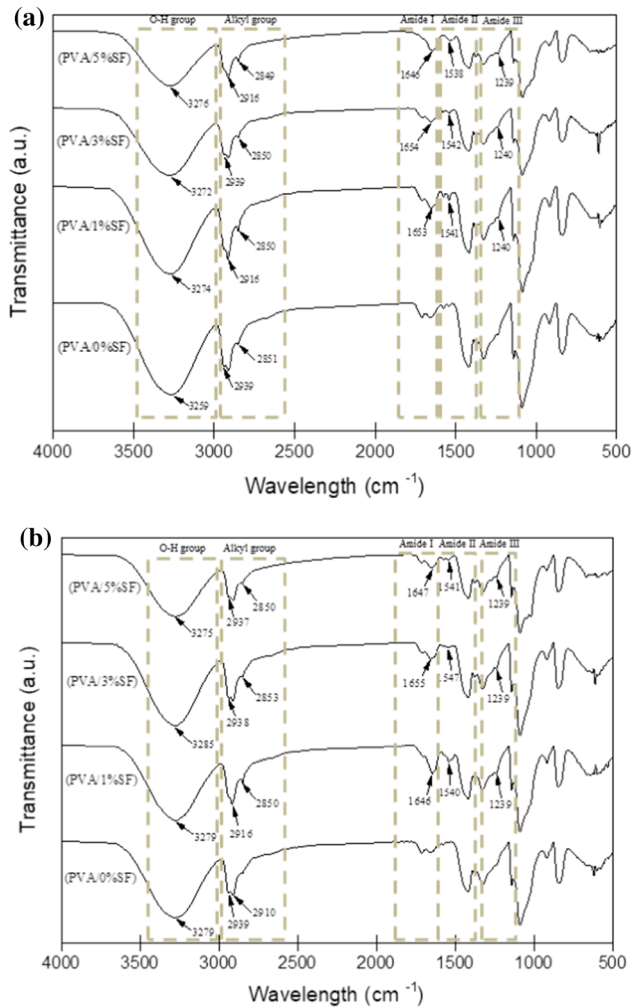
Figure 5 FTIR spectra of the biphasic scaffolds: **a** PVA/silk fibroin film and **b** PVA/silk fibroin sponge.
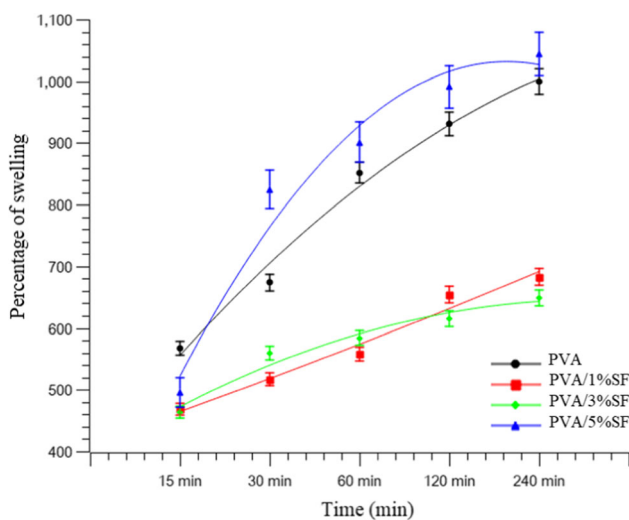

Figure 6 Swelling behavior of biphasic scaffolds: PVA, PVA/1%, 3%, and 5% SF.

proliferations increased from day 1 to day 3 in all scaffolds; however, the non-modified PVA scaffold had the lowest rate, and the PVA/3% SF scaffold showed higher proliferation than the PVA/1% SF scaffold but lower than the PVA/5% SF scaffold. However, at day 5, the PVA/5% SF scaffold showed a significantly lower proliferation rate than the PVA/3% SF scaffold. Proliferation of the PVA/3% SF scaffold was significantly higher than the other scaffolds. On day 7, however, fibroblast proliferations of the PVA/5% SF and PVA/3% SF scaffolds were not significantly different but significantly higher than the scaffolds of the pure PVA and PVA/1% SF. The pure PVA scaffold consistently exhibited the lowest fibroblast proliferation performance at all time points.

Osteoblast cell proliferation was measured at days 1, 3, 5, and 7 using the same reagent, PrestoBlue (Fig. 8b). Overall, an increasing trend from days 1 to 7 was observed. At day 1, no significant difference was observed among the groups. The PVA/5% SF scaffold showed a higher osteoblast proliferation than the PVA/3% SF and PVA/1% SF scaffolds at day 3. This difference was especially remarkable compared to the pure PVA scaffold. A similar trend was observed at day 5. The PVA/5% SF scaffold still showed a significantly higher rate of proliferation than the other scaffolds. However, the difference between the PVA/1% SF and PVA/3% SF scaffolds was not significantly different, but the proliferation rates of both the PVA/1% SF and 3% SF scaffolds were significantly higher than the pure PVA scaffold. At day 7, the PVA/5% SF scaffold once more expressed a significantly higher proliferation rate than the other scaffolds. Also, the PVA/3% SF scaffold had a significantly higher proliferation rate compared with the pure PVA scaffold. However, the difference in osteoblast cell proliferation rates between the PVA/1% SF and 3% SF scaffolds was not significantly different.

Discussion

Molecular organization in biphasic scaffolds

Molecular organization is one of the important clues in explaining the potential of scaffolds in their utilization in tissue engineering [43]. Some research has demonstrated that molecular organization,
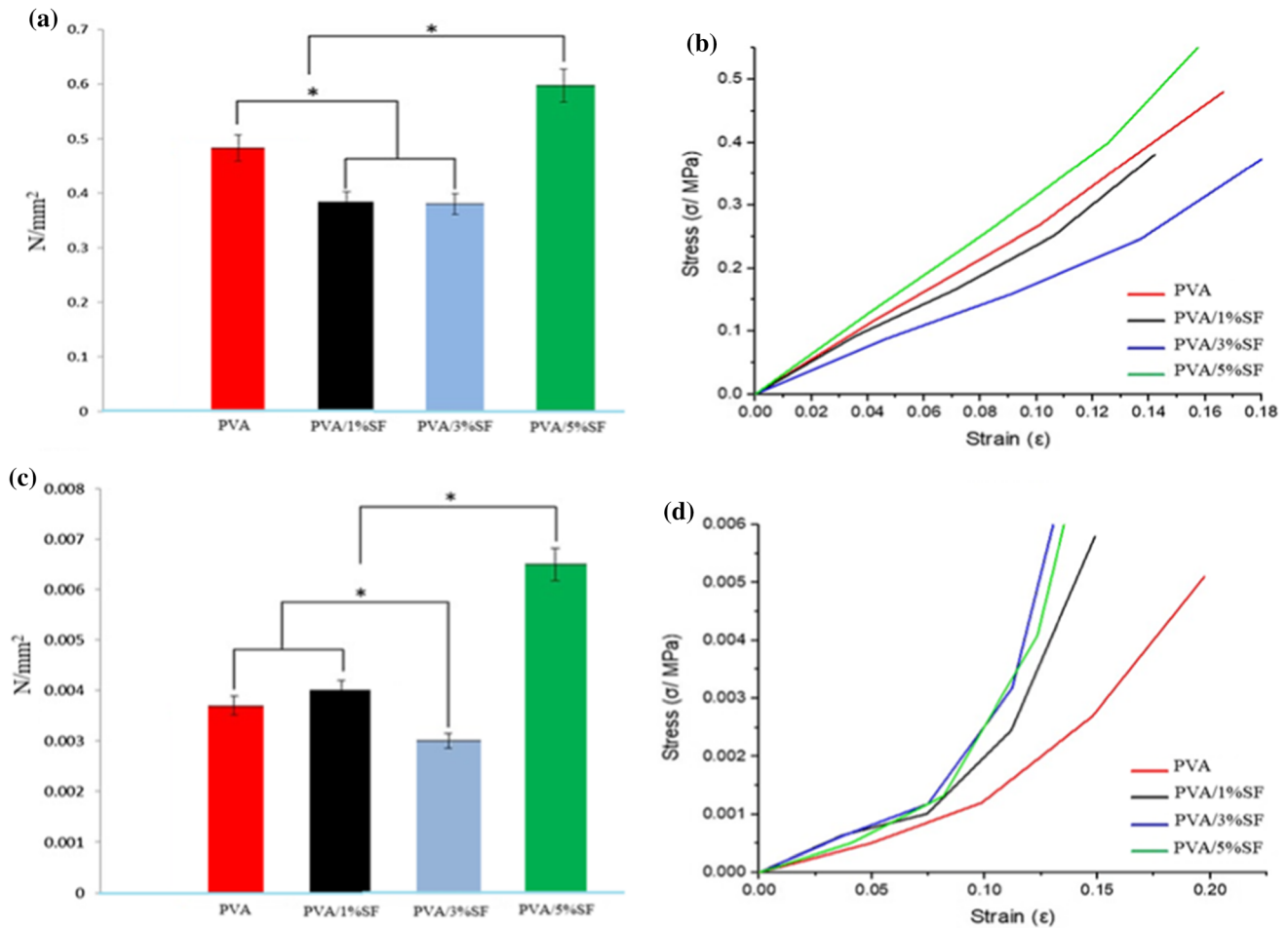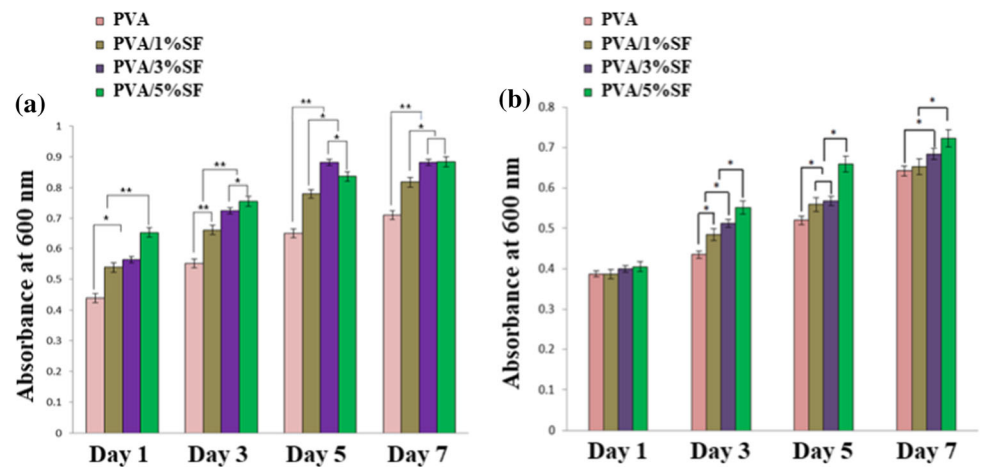
Figure 7 Compressive strengths and stress–strain curves of the biphasic scaffolds under dry **a** and **b** and wet **c** and **d** conditions.

Figure 8 Proliferation of fibroblasts cultured on PVA/silk fibroin films **a** and proliferation of osteoblasts cultured on PVA/silk fibroin sponge **b** measured with PrestoBlue reagent on days 1, 3, 5, and 7.

interaction, and mobility have an influence on the expression of the physical and mechanical stability of scaffold materials [44]. The stability of scaffold materials is an important facet of their performance in regulating new tissue formation [45]. In our

research, FTIR was selected to characterize molecular organization. FTIR characterization is related to the behavior of chemical groups of materials [46]. This refers to their molecular organization [47]. Some research has shown that molecular organization is

closely related to the structure of materials [48]. The PVA/silk fibroin film manufactured in this study demonstrated the molecular mobility of –OH groups and the interaction of the amide I, II, and III groups. This refers to the fact that there are two expressions of molecules, which are mobility and interaction that refer to the loose and dense structure formation, respectively, of scaffold materials [49, 50]. The mobility of the –OH group in our bioengineered material was mainly due to the molecules of PVA, whereas the interaction of the amide I, II, and III groups can be attributed to the SF molecules. The PVA/SF sponges manufactured in this research showed a molecular mobility of the –OH, amide I, II, and III groups, which indicated the loose structural formation of sponges [51].

Macrostructure of biphasic scaffolds related to mimicking materials design

The biphasic scaffolds in this research were formed via the micro-bubble technique. The macrostructure formation with this technique started with the micro-bubbles diffusing into the PVA + SF solution. At this step, the micro-bubbles were distributed into the solution. They were then trapped by PVA in the solution, and the solution with the micro-bubbles distributed was poured into the mold to form the biphasic scaffolds. At this step, the solution underwent phase separation. The first phase was characterized by the continuous polymer phase without non-continuous micro-bubbles at the bottom. The second phase was the continuous polymer phase with non-continuous micro-bubbles on the top. This phase-separated solution acted as the preform of the biphasic scaffolds. At the next step, the preform was solidified into biphasic scaffolds via freeze-drying. Finally, the biphasic scaffolds had their film layer connected to the sponge layer.

Our biphasic scaffolds which have the film layer connected to a sponge layer can be related to mimicking materials design that is suitable for tissue at the oral and maxillofacial area. Based on the gross anatomy, the oral and maxillofacial area shows a layer of soft tissue connected to the porous structure of bone tissue. The soft tissue is constructed mainly of an ECM membrane that serves as a scaffold for the cells of soft tissue. On the other hand, bone tissue is composed mainly of a 3D porous ECM that plays the role of a scaffold embedded with bone cells.

Importantly, this correlates well with our biphasic scaffolds based on mimicking materials design, which is similar to the gross anatomy of the oral and maxillofacial area. Furthermore, with materials production in mind, the biphasic macrostructure of our scaffolds was formed during fabrication. This is the attractive point suitable for scaling up the fabrication. This is an alternative choice for mass production of biphasic scaffolds.

Morphology of biphasic scaffolds related to mimicking materials design

In terms of the biphasic scaffolds fabricated in this study, the morphology of the film can be attributed to the micro-bubble fusion [52]. On the other hand, the sponge showed a homogenous structure composed of both main pores and sub-pores. The morphology of the film came from the collapse of micro-bubbles during fabrication [53]. This morphology acts as a barrier, which exhibits a suitable performance in preventing soft tissue invasion into the bone tissue during augmentation. As for the morphology of the sponge, the main pores resulted from the solidification of the micro-bubbles [54]. The sub-pores formed via the removal of the ice crystals during freeze-drying (Fig. 9) [55].

PVA with high amounts of SF demonstrated the presence of fibrils in the wall of the main pores. In particular, the PVA/5% SF scaffold showed a greater number of pores with fibrils than the other combinations because SF self-organizes into fibrils more readily in higher concentrations [56]. Our research demonstrated that the PVA/silk fibroin sponge possessed a structure that consisted of pores with fibrils. Importantly, the morphology afforded by the combination of pores and fibrils is suitable for the promotion of cell adhesion, proliferation, and migration, which enhances bone formation [57, 58].

Earlier research demonstrated that a homogenous structure with main pores and sub-pores is similar to the structure of bone [59]. Furthermore, research has shown that fibrils act as an ECM [60]. The sponge morphology of our scaffolds indicates the suitability of mimicking materials design to fabricate scaffolds with a structure similar to natural spongy bone. Similar to the macrostructure, the micro-formation of the porous structure was self-organized during fabrication. Our results demonstrated that biphasic scaffolds of PVA/SF fabricated by the micro-bubble
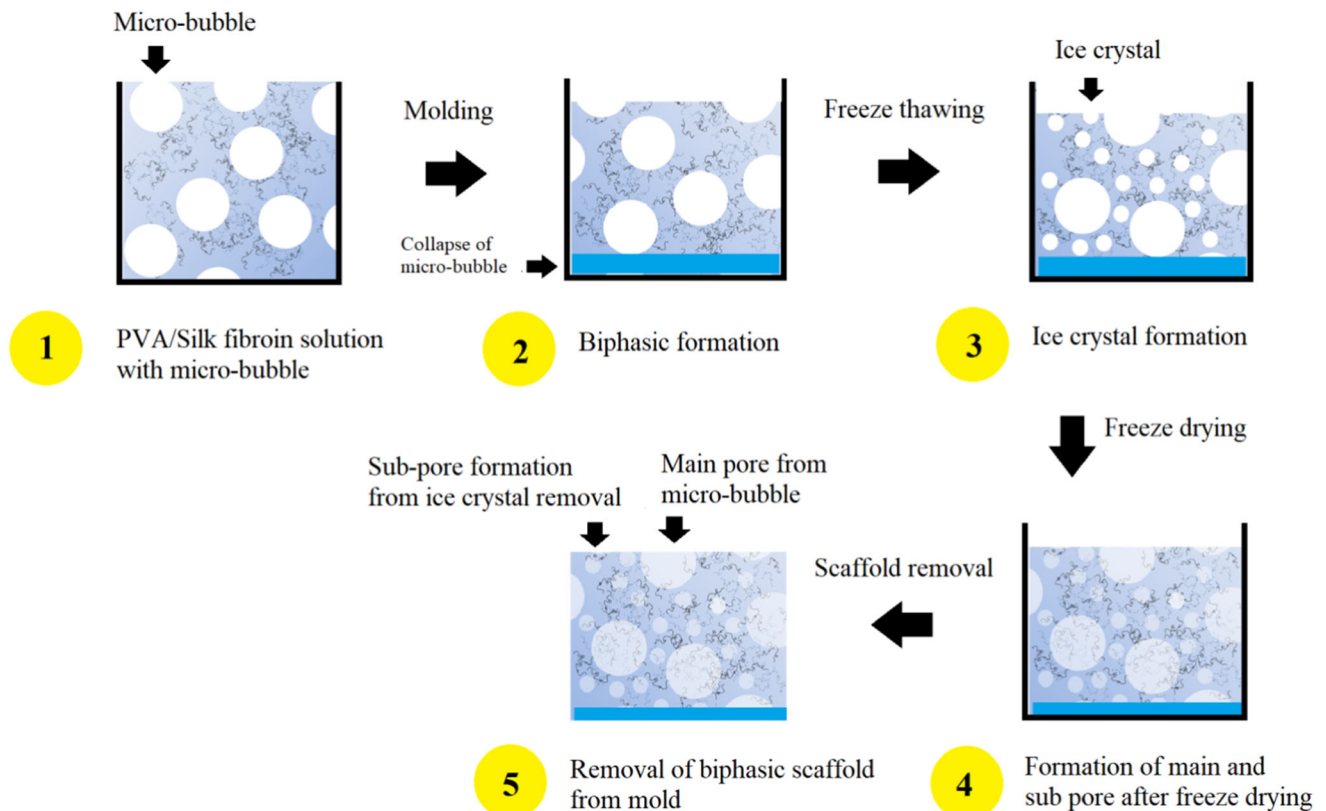
Figure 9 Proposed morphological formation of biphasic scaffolds.

technique incorporated with freeze-drying can form the self-organization of the macro- and microstructures, which is advantageous for mass production of biphasic scaffolds.

Evaluation of biphasic scaffolds related to performance of biomaterials

Our biphasic scaffolds were tested for their physical and mechanical properties as well as cell proliferation to evaluate and identify their application. Principally, swelling behavior is related to the diffusion of nutrients and biological signals that enhance the necessary cell behaviors leading to the promotion of tissue formation [61]. In our research, the PVA/5% SF combination showed the highest level of swelling due to the morphology of the pores with fibrils, which contributed to the swelling behavior. Furthermore, the film layer of the PVA/5% showed more molecular mobility of the –OH groups than the other scaffolds. This was related to the low molecular interaction between molecules, which led to the diffusion of water molecules that penetrated other molecules leading to the high level of swelling [62].

The mechanical properties are an important clue to understanding cell proliferation and play an important role in the promotion of issue formation [63]. Furthermore, suitable mechanical properties are needed to maintain both contour and shape during new tissue formation [7].

Meanwhile, some research has shown that cell proliferation is the clue biomarker related to the potential of a material in tissue engineering [64]. In particular, a high cell proliferation rate leads to a high level of tissue formation [65]. Therefore, cell proliferation was selected to serve mainly as a trigger related to the potential of our biphasic scaffolds. In our research, the film layer showed good fibroblast cell proliferation, which occurred because the film layer had a dense morphological structure with sufficient stability to support cell adhesion leading to enhancement of cell proliferation [66].

The morphology of the sponge layer had pores incorporated with fibrils, which is a suitable structure to support cell response, adhesion, spreading, migration, and proliferation [67, 68]. The fibrils facilitate cell adhesion and movement due to their structure [69], and the pores provide space for cell

proliferation. Some previous studies reported that different pore sizes are suitable for different cells which can be regulated into different tissue types [58, 70]. The pore size of bone tissue is about 300 μm which is suitable for osteoblast cell proliferation [71]. In our research, the pore size of the scaffolds was in the suitable range for promotion of cell proliferation, which is supported by previous studies.

The PVA/5% SF scaffold had the highest level of swelling, mechanical strength, and cell proliferation because of the unique pore morphology with fibrils

that could facilitate tissue formation. These are the good points of our biphasic biomaterial scaffolds.

Identification of applications for biphasic scaffolds in oral and maxillofacial surgery

According to the mimicking materials design, our biphasic scaffolds demonstrated a structure that had similar gross anatomy of a defect at the oral and maxillofacial area, particularly in areas that involve two phases of tissue: soft tissue and bone tissue. The biphasic scaffolds in this research presented the

Figure 10 Biphasic scaffolds proposed for oral and maxillofacial surgery. a Scaffolds for mandibular ridge augmentation and b scaffolds for alveolar cleft lip and palate repair.
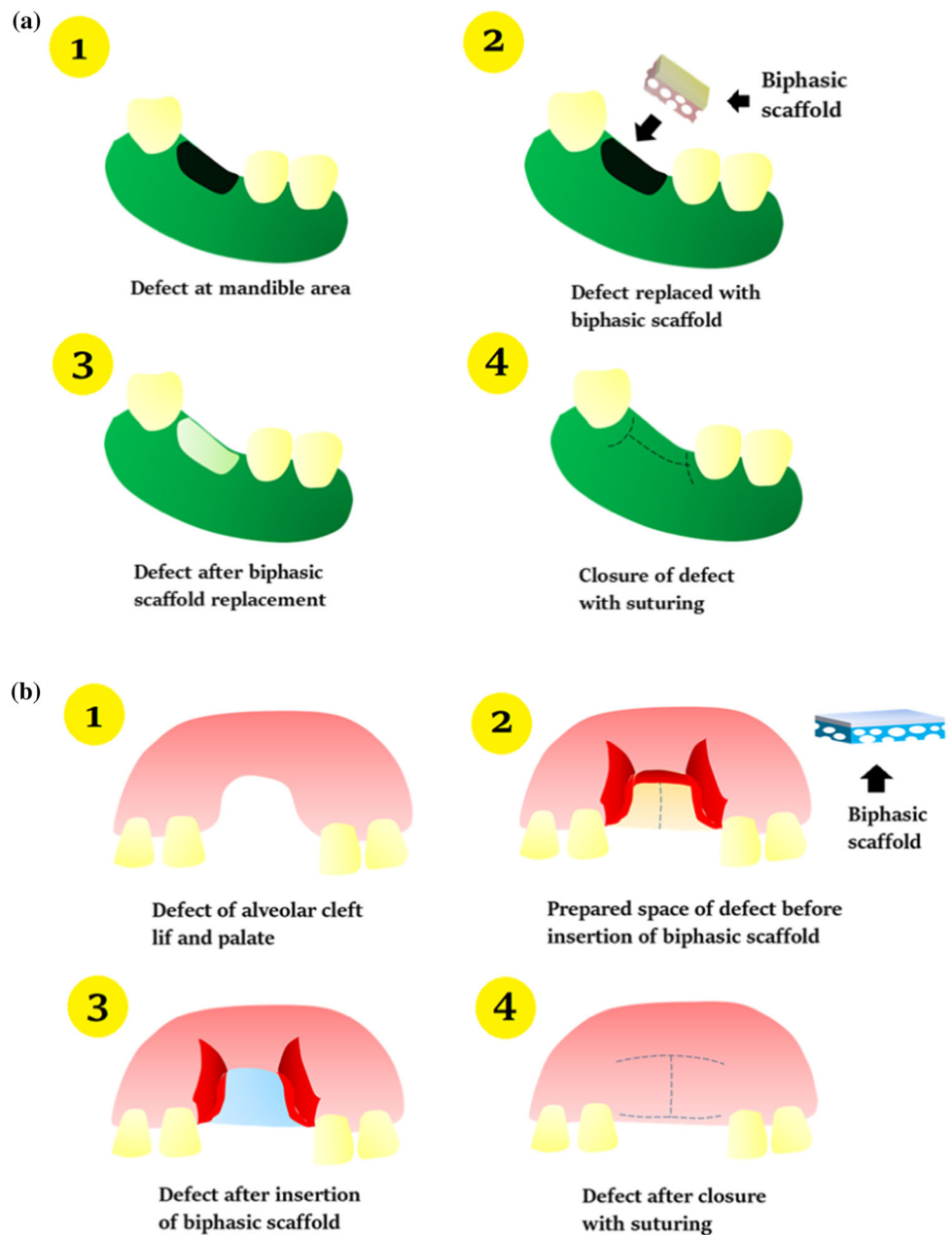
morphology of a sponge layer, which is similar to the ECM of spongy bone. This structure is suitable for repair of a tissue defect at the oral and maxillofacial area. Figure 10 illustrates examples for the application of biphasic scaffolds in oral and maxillofacial surgery for instance mandibular ridge augmentation and alveolar cleft lip and palate repair.

The first application of our biphasic scaffolds is for mandibular ridge augmentation as proposed in Fig. 10a. Bone loss repair can be performed by using grafting materials such as tri-calcium phosphate, hydroxyapatite, biphasic calcium phosphate, and calcium sulfate [72, 73]. The surgery protocol involves adding grafting material into the bone loss site before covering with a barrier membrane to prevent soft tissue invasion during augmentation. The defect is then closed by suturing. In reality, this protocol has many steps to complete the operation. Interestingly, our biphasic scaffolds have functions as a ready-to-use material: 1) to function as a barrier to prevent soft tissue invasion, which is the basic function of the film layer, 2) to promote bone formation based on the function of the sponge layer, and 3) to maintain contour shape at mandibular area without collapse during augmentation.

The second application involves the repair of alveolar cleft lip and palate as proposed in Fig. 10b. Some patients need surgery by adding bone grafting materials to the defect site before suturing. Similar to mandibular ridge augmentation, we propose our biphasic scaffolds for repair of alveolar cleft lip and palate to serve the functions to prevent soft tissue invasion, promote bone formation, and maintain the contour shape. Eventually, our biphasic scaffolds based on mimicking materials design show the performance as a ready-to-use material which is suitable for oral and maxillofacial surgery.

Conclusion

Biphasic scaffolds of polyvinyl alcohol with silk fibroin were fabricated based on mimicking materials design. We propose our scaffolds for oral and maxillofacial surgery. After fabrication, the biphasic scaffolds were characterized for their molecular and morphological formation, which is correlated with important properties related to the required functions suitable for oral and maxillofacial surgery. Our scaffolds demonstrated a structure based on mimicking

materials design. First, the macrostructure demonstrated a film layer in contact with a sponge layer, which is similar to the gross anatomy of a defect site environment of soft tissue and bone tissue. Second, a porous structure with fibrils was demonstrated in the sponge layer, which is similar to the ECM of spongy bone. Our scaffolds demonstrated based mimicking materials design matched with the requirements of a surgical approach. Furthermore, our research demonstrated an attractive choice for biphasic scaffold fabrication that showed structural self-organization at both the macro- and microscale similar to the natural complicated structure of bone including soft tissue. Our scaffolds exhibit their performance as a ready-to-use material with the properties needed for mandibular ridge augmentation and repair of alveolar cleft lip and palate. This also showed the possibility of scaling up the fabrication of biphasic scaffolds into mass production. Nevertheless, since the scope of our work was on the optimization of fabrication and the characterization and testing of the scaffolds, the results reflect the state of the art for applications in materials science. For future work, our scaffolds need in vivo testing to clarify biological performance that will concentrate on cell and molecular biology.

Declarations

Conflict of interest The authors declare that they have no conflict of interest.

References

[1] Tuna EB, Ozgen M, Cankaya AB, Sen C, Gencay K (2012) Oral rehabilitation in a patient with major maxillofacial trauma: a case management. Case Reports Dentistry 2012:1–5. https://doi.org/10.1155/2012/267143

[2] Lloyd, Stuart N., and William Cross. 2002. "European Urology Supplements The Current Use of Biomaterials in Urology." 1:4–8.

[3] Nguyen C, Young S, Kretlow JD, Mikos AG, Wong M (2011) Surface characteristics of biomaterials used for space maintenance in a mandibular defect: a pilot animal study. J Oral Maxillofac Surg 69(1):11–18. https://doi.org/10.1016/j.joms.2010.02.026

[4] Gobbi, SJ 2019. "Requirements for Selection/Development of a Biomaterial. Biomedical. J Sci Techn Res https://doi.org/10.26717/bjstr.2019.14.002554.

[5] Nuss KMR, von Rechenberg B (2008) Biocompatibility issues with modern implants in bone—a review for clinical orthopedics. Open Orthopaedics J 2(1):66–78. https://doi.org/10.2174/1874325000802010066

[6] Khan F, Tanaka M (2018) designing smart biomaterials for tissue engineering. Int J Mol Sci 19(1):1–14. https://doi.org/10.3390/ijms19010017

[7] O'Brien FJ (2011) Biomaterials & scaffolds for tissue engineering. Mater Today 14(3):88–95. https://doi.org/10.1016/S1369-7021(11)70058-X

[8] Roffi A, Krishnakumar GS, Gostynska N, Kon E, Candrian C, Filardo G (2017) The role of three-dimensional scaffolds in treating long bone defects: evidence from preclinical and clinical literature—a systematic review. Biomed Res Int 2017:1–13. https://doi.org/10.1155/2017/8074178

[9] Chocholata P, Kulda V, Babuska V (2019) "Fabrication of scaffolds for bone-tissue regeneration. Materials. https://doi.org/10.3390/ma12040568

[10] Henkel J, Hutmacher DW (2013) Design and Fabrication of Scaffold-Based Tissue Engineering. BioNanoMaterials 14(3–4):171–193. https://doi.org/10.1515/bnm-2013-0021

[11] Thavornyutikarn, Boonlom, Nattapon Chantarapanich, Kriskrai Sitthiseripratip, George A. Thouas, and Qizhi Chen. 2014. Bone Tissue Engineering Scaffolding: Computer-Aided Scaffolding Techniques. Vol. 3.

[12] Melek LN (2015) Tissue engineering in oral and maxillofacial reconstruction. Tanta Dental J 12(3):211–223. https://doi.org/10.1016/j.tdj.2015.05.003

[13] Kinoshita Y, Maeda H (2013) Recent developments of functional scaffolds for craniomaxillofacial bone tissue engineering Applications. Sci World J. https://doi.org/10.1155/2013/863157

[14] Panjapheree K, Kamonmattayakul S, Meesane J (2018) Biphasic scaffolds of silk fibroin film affixed to silk fibroin/chitosan sponge based on surgical design for cartilage defect in osteoarthritis. Mater Design 141:323–332. https://doi.org/10.1016/j.matdes.2018.01.006

[15] Thangprasert A, Tansakul C, Thuaksubun N, Meesane J (2019) Mimicked hybrid hydrogel based on Gelatin/PVA for tissue engineering in subchondral bone interface for osteoarthritis surgery. Mater Design 183:108113. https://doi.org/10.1016/j.matdes.2019.108113

[16] The 15th International Conference on Biomedical Engineering: ICBME 2013, 4th to 7th December 2013, Singapore; Goh, J., Ed.; IFMBE Proceedings; Springer International Publishing: Cham, 2014; Vol. 43. https://doi.org/10.1007/978-3-319-02913-9.

[17] Jamei E, Vrcelj Z (2021) Biomimicry and the built environment, learning from nature's solutions. Appl Sci 11(16):7514. https://doi.org/10.3390/app11167514

[18] Chen DA, Ross BE, Klotz LE (2015) Lessons from a coral reef: biomimicry for structural engineers. J Struct Eng 141(4):02514002

[19] Jalil WDA, Kahachi HAH (2019) The implementation of nano-biomimicry for sustainability in architecture. J Eng Sustain Develop 23(3):25–41. https://doi.org/10.31272/jeasd.23.3.3.

[20] Bar-Cohen, Yoseph. 2005. "Biomimetics: Mimicking and Inspired-by Biology." Smart Structures and Materials 2005: Electroactive Polymer Actuators and Devices (EAPAD) 5759:1. https://doi.org/10.1117/12.597436.

[21] Sangkert S, Kamolmatyakul S, Meesane J (2020) Mimicked scaffolds based on coated silk woven fabric with gelatin and chitosan for soft tissue defect in oral maxillofacial area. Int J Artif Organs 43(3):189–202. https://doi.org/10.1177/0391398819877191

[22] Lawrence BJ, Madihall SV (2008) Cell colonization in degradable 3D porous matrices basics of porous structures importance of spatial architecture. Cell Adh Migr 2(1):9–16

[23] Kumar A, Han SS (2017) PVA-based hydrogels for tissue engineering: a review. Int J Polym Mater PoN 66(4):159–182. https://doi.org/10.1080/00914037.2016.1190930

[24] Alexy P, Káchová D, Kršiak M, Bakoš D, Šimková B (2002) Poly(Vinyl Alcohol) stabilisation in thermoplastic processing. Polym Degrad Stabil 78(3):413–421. https://doi.org/10.1016/S0141-3910(02)00177-5

[25] Gaaz T, Sulong A, Akhtar M, Kadhum A, Mohamad A, Al-Amiery A (2015) Properties and applications of polyvinyl alcohol, halloysite nanotubes and their nanocomposites. Molecules 20(12):22833–22847. https://doi.org/10.3390/molecules201219884

[26] Sh AA, Henning S, Michler GH (2010) Polyvinyl alcohol–collagen–hydroxyapatite biocomposite nanofibrous scaffold: mimicking the key features of natural bone at the nanoscale level. Polymer 51(4):868–876. https://doi.org/10.1016/j.polymer.2009.12.046

[27] Teixeira, Marta A., M. Teresa P. Amorim, and Helena P. Felgueiras. 2020. "Poly (Vinyl Alcohol) -Based Nanofibrous Electrospun Sca Ff Olds for Tissue Engineering Applications."

[28] Sobczak-Kupiec A, Drabczyk A, Florkiewicz W, Głąb M, Kudłacik-Kramarczyk S, Słota D, Tomala A, Tyliszczak B (2021) Review of the applications of biomedical compositions containing hydroxyapatite and collagen modified by bioactive components. Mater. https://doi.org/10.3390/ma14092096

[29] Santosh Kumar BY, Isloor AM, Anil S, Venkatesan J, MohaKumar GC (2019) Calcium phosphate bioceramics with polyvinyl alcohol hydrogels for biomedical applications. Mater Res Exp. https://doi.org/10.1088/2053-1591/ab549f

[30] Maheshwari S, Uma K, Govindan M, Raja A, Pravin MBS, Vasanth Kumar S (2017) Preliminary studies of PVA/PVP Blends Incorporated with HAp and β- TCP bone ceramic as template for hard tissue engineering. Bio-Med Mater Eng 28(4):401–415. https://doi.org/10.3233/BME-171682

[31] Hou Q, Wang X, Ragauskas AJ (2019) Preparation and characterization of nanocellulose-polyvinyl alcohol multilayer film by layer-by-layer method. Cellulose 26(8):4787–4798. https://doi.org/10.1007/s10570-019-02413-0

[32] Nguyen TP, Nguyen QV, Nguyen VH, Le TH, Huynh VQN, Vo DVN, Trinh QT et al (2019) Silk fibroin-based biomaterials for biomedical applications: a review. Polymers 11(12):1933. https://doi.org/10.3390/polym11121933

[33] Pillai MM, Gopinathan J, Indumathi B, Manjoosha YR, Santosh Sahanand K, Dinakar Rai BK, Selvakumar R et al (2016) Silk–PVA hybrid nanofibrous scaffolds for enhanced primary human meniscal cell proliferation. J Membrane Biol 249(6):813–822. https://doi.org/10.1007/s00232-016-9932-z

[34] Melke J, Midha S, Ghosh S, Ito K, Hofmann S (2016) Silk fibroin as biomaterial for bone tissue engineering. Acta Biomater 31:1–16. https://doi.org/10.1016/j.actbio.2015.09.005

[35] Srinivasan R, Rose GD (1999) A physical basis for protein secondary structure. Proc Natl Acad Sci USA 96(25):14258–14263. https://doi.org/10.1073/pnas.96.25.14258

[36] Sun W, Gregory DA, Tomeh MA, Zhao X (2021) Silk fibroin as a functional biomaterial for tissue engineering. Int J Mol Sci 22(3):1–28. https://doi.org/10.3390/ijms22031499

[37] Kambe Y (2021) Functionalization of silk fibroin-based biomaterials for tissue engineering. Polym J. https://doi.org/10.1038/s41428-021-00536-5

[38] Johari N, Moroni L, Samadikuchaksaraei A (2020) Tuning the conformation and mechanical properties of silk fibroin hydrogels. Eur Polymer J 134(June):109842. https://doi.org/10.1016/j.eurpolymj.2020.109842

[39] Yao D, Liu H, Fan Y (2016) Silk scaffolds for musculoskeletal tissue engineering. Exp Biol Med (Maywood) 241(3):238–245. https://doi.org/10.1177/1535370215606994

[40] Lamlerd T, Soontornvipart K, Kesdangsakonwut S, Kanokpanont S, Damrongsakkul S (2017) In vivo bone regeneration of thai silk fibroin scaffolds with gelatin, hydroxyapatite and hyaluronic acid. Thai J Veterinary Med 47(2):165–172

[41] Li JJ, Kim K, Roohani-Esfahani SI, Guo J, Kaplan DL, Zreiqat H (2015) A biphasic scaffold based on silk and bioactive ceramic with stratified properties for osteochondral tissue regeneration. J Mater Chem B 3(26):5361–5376. https://doi.org/10.1039/c5tb00353a

[42] Kamalha E, Zheng YS, Zeng YC, Fredrick MN (2013) FTIR and WAXD study of regenerated silk fibroin. AMR 677:211–215. https://doi.org/10.4028/www.scientific.net/AMR.677.211

[43] Zhang H, Li L, Dai F, Zhang H, Ni B, Zhou W, Yang X, Wu Y (2012) Preparation and characterization of silk fibroin as a biomaterial with potential for drug delivery. J Transl Med 10(1):117. https://doi.org/10.1186/1479-5876-10-117

[44] Chen FM, Liu X (2016) Advancing biomaterials of human origin for tissue engineering. Prog Polym Sci 53:86–168. https://doi.org/10.1016/j.progpolymsci.2015.02.004

[45] Chan BP, Leong KW (2008) Scaffolding in tissue engineering: general approaches and tissue-specific considerations. Eur Spine 17(S4):467–479. https://doi.org/10.1007/s00586-008-0745-3

[46] Scaffolding Strategies for Tissue Engineering and Regenerative Medicine Applications. Materials 12 (11):1824. https://doi.org/10.3390/ma12111824.

[47] Faghihzadeh F, Anaya NM, Schifman LA, Oyanedel-Craver V (2016) Fourier transform infrared spectroscopy to assess molecular-level changes in microorganisms exposed to nanoparticles. Nanotechnol Environ Eng 1(1):1. https://doi.org/10.1007/s41204-016-0001-8

[48] Hofko B, Alavi MZ, Grothe H, Jones D, Harvey J (2017) Repeatability and sensitivity of FTIR ATR spectral analysis methods for bituminous binders. Mater Struct 50(3):187. https://doi.org/10.1617/s11527-017-1059-x

[49] Bai M, Qin G, Sun Z, Long G (2015) Relationship between molecular structure characteristics of feed proteins and protein in vitro digestibility and solubility. Asian Australas J

Anim Sci 29(8):1159–1165. https://doi.org/10.5713/ajas.15.0701

[50] Liu Q, Wang F, Gu Z, Ma Q, Hu X (2018) Exploring the structural transformation mechanism of chinese and thailand silk fibroin fibers and formic-acid fabricated silk films. IJMS 19(11):3309. https://doi.org/10.3390/ijms19113309

[51] Tretinnikov ON, Zagorskaya SA (2012) Determination of the degree of crystallinity of poly (Vinyl Alcohol) by FTIR spectroscopy. J Appl Spectrosc 79(4):521–526. https://doi.org/10.1007/s10812-012-9634-y

[52] Niu C, Li X, Wang Y, Liu X, Shi J, Wang X (2019) Design and performance of a poly (Vinyl Alcohol)/silk fibroin enzymatically crosslinked semi-interpenetrating hydrogel for a potential hydrophobic drug delivery. RSC Adv 9(70):41074–41082. https://doi.org/10.1039/C9RA09344C

[53] Brittle S, Desai P, Ng WC, Dunbar A, Howell R, Tesař V ZWB (2015) Minimising microbubble size through oscillation frequency control. Chem Eng Res Des 104:357–366. https://doi.org/10.1016/j.cherd.2015.08.002

[54] Kantarci N, Borak F, Ulgen KO (2004) Bubble Column Reactors. Process Biochem-US 40(7):2263–2283. https://doi.org/10.1016/j.procbio.2004.10.004

[55] Parivatphun T, Nooklay B, Kokoo R, Meesane J, Kooptarnond K, Khangkhamano M (2019) Fabrication of bioscaffolds using bubbling technique for bone tissue engineering. MSF 962:125–128. https://doi.org/10.4028/www.scientific.net/MSF.962.125

[56] Haugh MG, Murphy CM, O'Brien FJ (2010) Novel freeze-drying methods to produce a range of collagen-glycosaminoglycan scaffolds with tailored mean pore sizes. Tissue Eng Part C-Me 16(5):887–894. https://doi.org/10.1089/ten.tec.2009.0422

[57] Sangkert S, Meesane J, Kamonmattayakul S, Chai WL (2016) Modified silk fibroin scaffolds with collagen/decellularized pulp for bone tissue engineering in cleft palate: morphological structures and biofunctionalities. Mat Sci Eng C-Mater 58:1138–1149. https://doi.org/10.1016/j.msec.2015.09.031

[58] Bružauskaitė I, Bironaitė D, Bagdonas E, Bernotienė E (2016) Scaffolds and cells for tissue regeneration: different scaffold pore sizes—different cell effects. Cytotechnology 68(3):355–369. https://doi.org/10.1007/s10616-015-9895-4

[59] Abbasi N, Hamlet S, Love RM, Nguyen NT (2020) Porous scaffolds for bone regeneration. J Sci Adv Mater Devic 5(1):1–9. https://doi.org/10.1016/j.jsamd.2020.01.007

[60] Turnbull G, Clarke J, Picard F, Riches P, Jia L, Han F, Li B, Shu W (2018) 3D bioactive composite scaffolds for bone tissue engineering. Bioact Mater 3(3):278–314. https://doi.org/10.1016/j.bioactmat.2017.10.001

[61] Vigier S, Fülöp T (2016) Exploring the Extracellular Matrix to Create Biomaterials. In Composition and Function of the Extracellular Matrix in the Human Body; Travascio, F., Ed.; InTech, https://doi.org/10.5772/62979.

[62] Zhu J, Marchant RE (2011) Design properties of hydrogel tissue-engineering scaffolds. Expert Rev Med Devic 8(5):607–626. https://doi.org/10.1586/erd.11.27

[63] Chen M, Coasne B, Guyer R, Derome D, Carmeliet J (2018) Role of hydrogen bonding in hysteresis observed in sorption-induced swelling of soft nanoporous polymers. Nat Commun 9(3507):1–7. https://doi.org/10.1038/s41467-018-05897-9

[64] Vining KH, Mooney DJ (2017) Mechanical forces direct stem cell behaviour in development and regeneration. Nat Rev Mol Cell Biol 18(12):728–742. https://doi.org/10.1038/nrm.2017.108

[65] Parivatphun T, Sangkert S, Meesane J, Kokoo R, Khangkhamano M (2020) Constructed microbubble porous scaffolds of polyvinyl alcohol for subchondral bone formation for osteoarthritis surgery. Biomed Mater (Bristol). https://doi.org/10.1088/1748-605X/ab99d5

[66] Beloti MM, Rosa AL (2005) Osteoblast differentiation of human bone marrow cells under continuous and discontinuous treatment with dexamethasone. Braz Dent J 16(2):156–161. https://doi.org/10.1590/S0103-64402005000200013

[67] Tonazzini I, Bystrenova E, Chelli B, Greco P, Stoliar P, Calo A, Lazar A, Borgatti F, D'Angelo P, Martini C, Biscarini F (2010) Multiscale morphology of organic semiconductor thin films controls the adhesion and viability of human neural cells. Biophys J 98(12):2804–2812. https://doi.org/10.1016/j.bpj.2010.03.036

[68] Xie J, Bao M, Bruekers SMC, Huck WTS (2017) Collagen gels with different fibrillar microarchitectures elicit different cellular responses. ACS Appl Mater Interfaces 9(23):19630–19637. https://doi.org/10.1021/acsami.7b03883

[69] Le P, Mai-Thi HN, Stoldt VR, Tran NQ, Huynh K (2021) Morphological dependent effect of cell-free formed supramolecular fibronectin on cellular activities. Biol Chem 402(2):155–165. https://doi.org/10.1515/hsz-2019-0402

[70] Dalton, Caleb J., and Christopher A. Lemmon. 2021. Fibronectin: molecular structure, fibrillar structure and mechanochemical signaling.

[71] Loh QL, Choong C (2013) Three-dimensional scaffolds for tissue engineering applications: role of porosity and pore size. Tissue Eng Part B: Rev 19(6):485–502. https://doi.org/10.1089/ten.teb.2012.0437

[72] Wo J, Huang SS, Dong Ying Wu, Zhu J, Li ZZ, Yuan F (2020) The Integration of pore size and porosity distribution on Ti-6A1–4V Scaffolds by 3D Printing in the modulation of

Osteo-Differentation. J Appl Biomater Funct Mater. https://doi.org/10.1177/2280800020934652

[73] Ohe JY, Kim GT, Lee JW, Nawas BA, Jung J, Kwon YD (2016) Volume stability of hydroxyapatite and β-tricalcium phosphate biphasic bone graft material in maxillary sinus floor elevation: a radiographic study using 3D cone beam computed tomography. Clin Oral Implant Res 27(3):348–353. https://doi.org/10.1111/clr.12551

[74] de Grado F, Gabriel LK, Idoux-Gillet Y, Wagner Q, Musset AM, Benkirane-Jessel N, Bornert F, Offner D (2018) Bone substitutes: a review of their characteristics, clinical use, and perspectives for large bone defects management. J Tissue Eng. https://doi.org/10.1177/2041731418776819

Publisher's Note Springer Nature remains neutral with regard to jurisdictional claims in published maps and institutional affiliations.